A Novel Approach for the Analysis of Electromagnetic Field with Rotating Body

Shafrida Sahrani [1], Hiroshi Iwamatsu [2], and Michiko Kuroda [3]

[1] Graduate School of Bionics, Computer and Media Science
[3] School of Computer Science
Tokyo University of Technology, Hachioji, 192-0982 Tokyo, Japan
sshafrida@feng.unimas.my, kuroda@cs.teu.ac.jp

[2] College of Science and Technology
Nihon University, Chiyoda, 101-8308 Tokyo, Japan

Abstract ─ In this paper, a novel approach which combines the FDTD method with overset grid generation method is proposed for the analysis of the EM field with rotating body. The analysis is carried out together with the Lorentz transformation to comprise with the higher velocity cases. To apply the Lorentz transformation to the FDTD method, at least two frames are required, and we primitively modelled it with the overset grid generation method. With the Lorentz transformation, the time component changes at each of the grid point. The time component that has been changed by Lorentz transformation must be fixed as the numerical procedure. Through the interpolation technique, it is possible to fix the time component easily. We have previously proposed this novel approach for a stationary and uniformly moving body. Here, this analysis is further expanded and has included a more detailed discussion of the EM field interactions in a rotating environment. The numerical results show the characteristics of the EM field when the incident wave strikes the rotating body. For validation, the numerical results are compared with the theoretical results, and good agreements were obtained. The proposed novel approach has shown its consistency over higher relative velocity cases.

Index Terms ─ FDTD method, Lorentz transformation, moving boundary problems, overset grid generation method, relative motion, rotating body.

I. INTRODUCTION

The analytical theory of the electromagnetic (EM) field with moving bodies is an emerging topic of interest to treat various solution of engineering problems [1-2]. This has spurred the development of an appropriate numerical technique concerning EM wave interactions with the complex and dynamic moving boundaries [3-5]. This paper introduces a novel numerical approach for the analysis of the EM field with the presence of a rotating body by overset grid generation method with the aim of combining the advantages of finite-difference time-domain (FDTD) method and the Lorentz transformation.

A conventional Lorentz transformation [6] in special relativity requires at least two frames of reference when applied to the FDTD method. The overset grid generation method has made it possible to employ the two frames as an effort to create a compact and efficient numerical approach. The overset grid generation method has been used mainly in computational fluid dynamics (CFD) for treating problems in complex, dynamically moving geometries [7-8]. This method offers an effective way to combine multiple meshes into a set of single mesh. The implementation of the Lorentz transformation to the method gives an advantage to integrate with the moving component in the EM fields for higher velocity values. In Lorentz transformation, the time component

changes at each of the grid points. However, the FDTD method requires the value of the EM field correspond to each time component. To calculate the FDTD method, the changing time component in the Lorentz transformation is fixed through an interpolation scheme. This allows a coherent point in time and space component with the FDTD method.

In the previous paper, the proposed novel approach has shown promising possibilities in providing accurate solutions for a stationary and uniformly moving body [9]. This paper will address the extension of the novel approach to treat the EM field interactions in a rotating environment. The numerical results indicate the modulations and the characteristics of the EM field when the incident wave strikes the rotating body. The proposed novel approach has shown its advantage over higher velocity cases. In addition, its validity has been demonstrated in comparison between the numerical results and the theoretical results. The observed waveforms are found to be in good agreement with the theoretical results. The consistency of this numerical approach has made it possible in providing a strong numerical support for developing high-speed optical devices and, also, in application of carbon nanotubes [10-11].
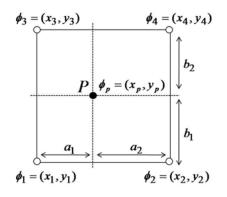
II. OVERVIEW OF OVERSET GRID GENERATION METHOD

Fig. 1. Interpolation model.

The use of overset grid generation method arose from the need to provide a simple computational method in handling complex stationary and/or moving geometries [12]. Basically, the overset grid generation method consists of a main mesh and sub-meshes. The sub-

mesh is allowed to overlap on the main mesh in an arbitrary manner. The main mesh covers the entire computational domain while the movable sub-mesh acts as a component mesh. With this approach, the sub-mesh is used to model complex stationary and/or dynamically moving geometries.

At any overset boundary, each of the grid components in the sub-mesh can be calculated independently from the overlapped main mesh. This approach requires interpolation routines to transmit the data between both meshes. Figure 1 describes the data transfer between the overlapped meshes by the linear interpolation algorithm. The unknown value ϕ_p, at point P in the main mesh (dashed line) can be determined from the existing factors $\phi_1, \phi_2, \phi_3, \phi_4$ in the sub-mesh (solid line) as in Eq.(1):

$$\phi_p = \frac{(\phi_1 \times a_2 + \phi_2 \times a_1) \times b_2 + (\phi_3 \times a_2 + \phi_4 \times a_1) \times b_1}{(a_1 + a_2)(b_1 + b_2)} \quad . \quad (1)$$

The value at the interpolation point is used to transfer inter-grid information and recomputed at each time step. The finer resolution in the overlapped region with sufficient inter-grid ratio gives a better computational accuracy. The key advantage of this method lies in the simplicity of the concept and its ability to calculate large scale or longer distance of motion.

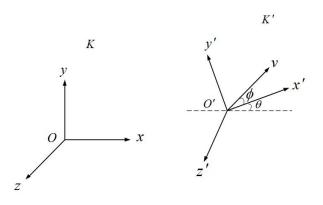## III. LORENTZ TRANSFORMATION FOR THE FDTD METHOD

Fig. 2. Two inertial frames in relative motion.

Lorentz transformation provides a relation for space and time components between the coordinates of two inertial observers [13]. Figure 2

shows the basic Lorentz transformation in relative motion. Assume there are two observers, O and O' in each frame K and K'. Observer O is in the (x, y, z, t) axis and O' is in the (x', y', z', t') axis at angular, θ against the axis in frame K. The observer O' is assumed to move against the observer O in the direction ϕ, with relative velocity, $\mathbf{v}$ (m/s). When the observer O' is at time t', Lorentz transformation can be described as:

$$dr' = \gamma(d\mathbf{r} - \mathbf{v}dt) + (\gamma - 1)\frac{\mathbf{v} \times \mathbf{v} \times d\mathbf{r}}{v^2} \qquad (2)$$

$$dt' = \gamma\left(dt - \frac{\mathbf{v} \bullet d\mathbf{r}}{c^2}\right) , \qquad (3)$$

where $\gamma = 1/\sqrt{1 - v^2/c^2} = 1/\sqrt{1 - \beta^2}$. The vector for the space component in the Lorentz transformation is defined as $\mathbf{r} = \mathbf{r}(x, y, z)$ and $\mathbf{r}' = \mathbf{r}'(x', y', z')$. The transition from the observer O' to O is obtained by replacing $\mathbf{v}$ in Eq. (2) and Eq. (3) to $-\mathbf{v}$. Hence, $d\mathbf{r}'$, dt' to $d\mathbf{r}$ and dt, respectively. This theory satisfies all possible range of relative velocity.

Lorentz transformation for the EM field can be described as in Eq. (4a) - Eq. (4d) [14].

$$\mathbf{E}' = \mathbf{E}_{\parallel} + \gamma(\mathbf{E} + \mathbf{v} \times \mathbf{B})_{\perp} \qquad (4a)$$

$$\mathbf{H}' = \mathbf{H}_{\parallel} + \gamma(\mathbf{H} - \mathbf{v} \times \mathbf{D})_{\perp} \qquad (4b)$$

$$\mathbf{D}' = \mathbf{D}_{\parallel} + \gamma\left(\mathbf{D} + \frac{\mathbf{v} \times \mathbf{H}}{c^2}\right)_{\perp} \qquad (4c)$$

$$\mathbf{B}' = \mathbf{B}_{\parallel} + \gamma\left(\mathbf{B} - \frac{\mathbf{v} \times \mathbf{E}}{c^2}\right)_{\perp} . \qquad (4d)$$

$\mathbf{E}_{\parallel}, \mathbf{H}_{\parallel}, \mathbf{D}_{\parallel}, \mathbf{B}_{\parallel}$ and $\mathbf{E}_{\perp}, \mathbf{H}_{\perp}, \mathbf{D}_{\perp}, \mathbf{B}_{\perp}$ are the parallel and perpendicular components for the EM field against the moving direction.
For the present work, EM field interaction with moving boundaries is investigated by using the FDTD method. It is important to note that the space and the time component in the basic FDTD method are obtained at alternate half-time steps to evaluate the EM field [15-16]. However, the time component in the Lorentz transformation changes at each grid point. The restriction in the space and time component from the Lorentz transformation and FDTD method can be solved with the advantage of the overset grid generation method.

The time components that were changed in the Lorentz transformation are fixed by using the linear interpolation scheme.
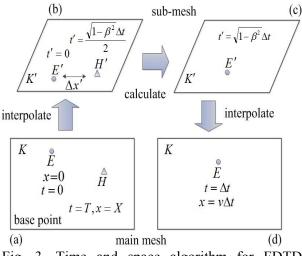

Fig. 3. Time and space algorithm for FDTD method and Lorentz transformation by overset grid generation method.

Figure 3 illustrates the diagram of the proposed computational algorithm based on the time and the space algorithm in the FDTD method and the Lorentz transformation. In actual algorithmic program, the sub-mesh is overlap on the main mesh in an arbitrary manner. For explanation purposes, the sub-mesh and the main mesh are depicted separately. Figures 3(a) and 3(d) are assumed to be the main mesh, while, Figs. 3(b) and Fig. 3(c) describe the sub-mesh. First, the position of the sub-mesh on the main mesh is identified in the algorithm. Then, the EM field components on the main mesh in Fig. 3(a) are interpolated to the field components on the moving sub-mesh in Fig. 3(b) by applying the Lorentz transformation. Here, the electric field is calculated in both meshes by the FDTD method. The flow of the algorithm mentioned above is shown from Fig. 3(a) to Fig. 3(c). The calculated value of the electric field at the sub-mesh in Fig. 3(c) is interpolated back to the main mesh in Fig. 3(d) through Lorentz transformation. Here, the half time increment is advanced. At time $t = \Delta t$ in the main mesh, the value for the time component on the moving sub-mesh in Fig. 3(c) should be:

$$t' = \sqrt{1 - v^2/c^2}\,\Delta t \quad . \qquad (5)$$

To obtain the electric field, E at $t = \Delta t$, $x = v\Delta t$ in Fig. 3(d), it is necessary to interpolate the time component to denote $t = T$ at $x = X$ in Fig. 3(a). The values for T and X can be obtained from the inverse Lorentz transformation, given by $T = \gamma\left(t' + x'v/c^2\right)$ and $X = \gamma\left(x' + vt'\right)$. Here, the time component of the magnetic field, H' in Fig. 3(b) is:

$$t' = \sqrt{1 - v^2/c^2}\, \Delta t/2 . \qquad (6)$$

In the derivation of Eq. (6), the same process is iterated to calculate the magnetic field. This process continues until the time-stepping is concluded. This permits the FDTD method to provide numerical models of wave interactions with the moving body accurately.

IV. NUMERICAL MODELLING AND RESULTS
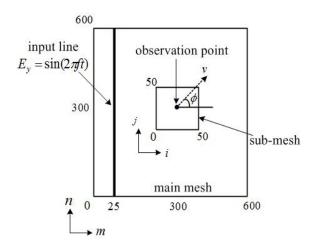
A. Validation of the Lorentz transformation

Fig. 4. Numerical model.

Figure 4 illustrates the numerical model to evaluate the advantages of the novel approach. Here, the moving sub-mesh, is overlapped on the static main mesh. The main mesh is set to 600×600 grids and the sub-mesh is 50×50 grids. These grids are terminated with Mur's absorbing boundary conditions [17]. The space increment for the main mesh is $\Delta x_m = \Delta y_m = \lambda/60$, and for the

sub-mesh is $\Delta x_s = \Delta y_s = \lambda/60$. λ is the wavelength of the incident wave. The incident wave is a sinusoidal plane wave with the input frequency, $f_0 = 100 (GHz)$. The input frequency is at $m = 25$ on the main mesh. The observation point is set at the point $(25, 25)$ on the sub-mesh. The sub-mesh is assumed to move with angular, ϕ, with relative velocity, $v(m/s)$. The time step, Δt in this analysis is set to $5.0 \times 10^{-14}(s)$, as to meet the courant condition, $c \leq \dfrac{\Delta x}{\Delta t}$, where c is the velocity of light and Δx is the space increment.

Figure 5 shows the comparison of the numerical results with the theoretical results for the normalized velocity versus normalized amplitude of electric field, $E'_z (V/m)$. Here, the sub-mesh is assumed to move for $\phi = \pi$, where the observation point is approaching towards the incident waves. The theoretical result is calculated based on Eq. (7) [18].

$$\frac{E'}{E_0} = \sqrt{\frac{1 + v/c}{1 - v/c}} , \qquad (7)$$

where v is the velocity of the motion and c is the speed of light. From Fig. 5, the observed waveforms are found to be in good agreement with the theoretical results in high relative velocities, up to $v = 0.9c$ closed with the finite speed of light. The consistency of this novel approach with implementation of Lorentz transformation shows its potential in providing an accurate numerical solution for the EM field in moving boundaries.
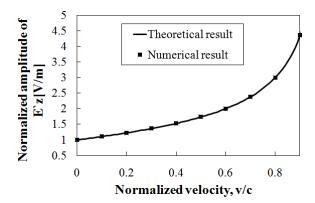

Fig. 5. Comparison of theoretical and numerical results.

B. Moving surface in a rotating environment

This paper further proposes the novel numerical approach to treat the EM field interaction with the rotating body. Considering the Lorentz transformation in a rotating environment, the observer O' is assumed to rotate with angular θ against the observer O with relative velocity, $\mathbf{v}$ (m/s). Under the rotation of the coordinate system, as shown in Fig. 6, the cross product for vector in Eq. (4a) and Eq. (4b) can be defined as:

$$\mathbf{v} \times \mathbf{B} = (B_{sz} v \sin\phi, -B_{sz} v \cos\phi, 0) \tag{8}$$

$$\mathbf{v} \times \mathbf{D} = (0, 0, D_{sy} v \cos\phi - D_{sx} v \sin\phi) , \tag{9}$$

where ϕ is a position of the angle in the EM field. The vector for parallel and perpendicular components against the moving direction in Eq. (4a) to Eq. (4d) can be derived as:

$$E_{\parallel} = \mathbf{u}_{\parallel} \bullet \mathbf{E} \tag{10a}$$

$$E_{\perp} = \mathbf{u}_{\perp} \bullet \mathbf{E} \tag{10b}$$

$$H_{\parallel} = \mathbf{u}_{\parallel} \bullet \mathbf{H} \tag{11a}$$

$$H_{\perp} = \mathbf{u}_{\perp} \bullet \mathbf{H} , \tag{11b}$$

where $\mathbf{u}_{\parallel}$ and $\mathbf{u}_{\perp}$ is given by

$$\mathbf{u}_{\parallel} = (\cos\phi, \sin\phi, 0) \tag{12a}$$

$$\mathbf{u}_{\perp} = (-\sin\phi, \cos\phi, 0) . \tag{12b}$$

Here, the analysis is carried out for the transverse electric (TE) case to investigate wave interactions with the rotating body. For 2D cases, the electric field for the static main mesh in x, y
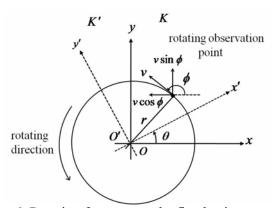
direction is described as $E_m = (E_{mx}, E_{my}, 0)$, while, the rotating sub-mesh in the x', y' direction is defined as $E_s = (E_{sx}, E_{sy}, 0)$. Thus, the electric field in the Lorentz transformation for the main mesh and the sub-mesh can be described as $E'_m = (E'_{mx}, E'_{my}, 0)$ and $E'_s = (E'_{sx}, E'_{sy}, 0)$, respectively with velocity, $v = (v \cos\phi, v \sin\phi, 0)$. The vector of TE waves for 2D rotating sub-mesh can be written as in Eq. (13) to Eq. (15):

$$\mathbf{E}_{sx} = \mathbf{E}_{mx} \cos\theta + \mathbf{E}_{my} \sin\theta \tag{13}$$

$$\mathbf{E}_{sy} = -\mathbf{E}_{mx} \sin\theta + \mathbf{E}_{my} \cos\theta \tag{14}$$

$$\mathbf{H}_{sz} = \mathbf{H} , \tag{15}$$

where $\theta = \omega t$. ω is the angular velocity. Hence, the Lorentz transformations of the EM fields in a rotating environment are given by:

$$\mathbf{E}'_x = \mathbf{E}'_{\parallel} \cos(-\phi) + \mathbf{E}'_{\perp} \sin(-\phi) \tag{16}$$

$$\mathbf{E}'_y = -\mathbf{E}'_{\parallel} \sin(-\phi) + \mathbf{E}'_{\perp} \cos(-\phi) \tag{17}$$

$$\mathbf{H}'_z = \mathbf{H}' . \tag{18}$$

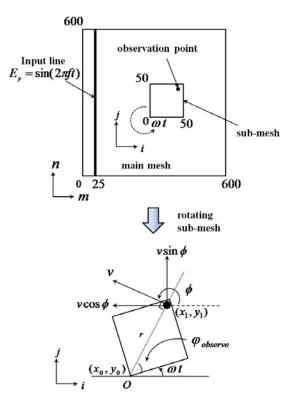Fig. 6. Rotating frame around a fixed axis.

Fig. 7. Numerical model for rotating sub-mesh.

Figure 7 illustrates the numerical model for the rotating sub-mesh on the overlapped main mesh. The grid numbers for the main mesh are 600×600 grids and 50×50 grids for the sub-mesh. In this analysis, the observation point is at the point (45,45) on the sub-mesh. Initially, the sub-mesh is assumed to rotate in a counter clockwise direction with relative angular velocity, ω. The incident waves is sinusoidal plane wave with input frequency, $f_0 = 100 (GHz)$, and given on the static main mesh at, $m = 25$. The centre of a rotating point O is fixed at the point (0,0) on the sub-mesh. The velocity, v for the EM field is given by $v = \omega r$, which is related to the angular velocity depending on the distance from the centre of rotation to the observation point, r. In actual analysis, $r = 3.18 \times 10^{-3} (m)$ is obtained from the derivation of the equation, $r = \sqrt{(x_1 - x_0)^2 + (y_1 - y_0)^2}$. The rotating angle in the EM field, ϕ, can be calculated by $\phi = \dfrac{\pi}{2} + \omega t + \varphi_{observe}$, where $\varphi_{observe}$ is the angle of the observation point from the fixed rotation centre on the sub-mesh. The value for $\varphi_{observe}$ is derived from the equation, $\varphi_{observe} = \arccos(x_1 - x_0 / r)$, where x_0 and x_1 is the fixed rotating point and the observation point of the EM field in x - axis on the sub-mesh, respectively. The time increment, Δt in this analysis is set to $5.0 \times 10^{-14} (s)$. The numerical results for EM wave interactions in rotating environment are shown in Fig. 8, Fig. 9 and Fig. 10.

Figure 8 shows the modulation of the received waveform for the magnetic field, $H_z' (V/m)$ at angular velocity, $\omega = 0.86 \times 10^{10} (rad/\sec)$, and velocity, $v = 2.73 \times 10^7 (ms^{-1})$. The starting time of the rotation is observed at 2000 time steps. The dotted line illustrates the theoretical results for the normalized amplitude of H_z'. The theoretical result is given by Eq. (19), accommodate with the existing theory [19].

$$\frac{H_z'}{H_0} = \sqrt{\frac{1 + v/c \cos\theta}{1 - v/c \cos\theta}} \quad . \tag{19}$$

The comparison data of the numerical results and the theoretical results is shown in Table 1. The data shows the observed waveforms are found to be in good agreement when compared with the theoretical results.

Figures 9(a) and 9(b) illustrates the modulation of the received waveform for E_x' and E_y', respectively. The modulation waveform demonstrates the wave interactions when the rotated observation point is approaching or rotating far away from the incident wave. Here, the sub-mesh starts its counter clockwise rotation at 2000 time steps with the angular velocity, $\omega = 2.14 \times 10^{10} (rad/\sec)$ and the velocity, $v = 6.81 \times 10^7 (ms^{-1})$. The modulation waveform demonstrates large wave amplitude with shorter frequency when the observation point is rotated towards the incident wave. Meanwhile, the wave amplitude is slightly shorter with longer frequency when the observed point is rotated away from the incident wave. The rotating sub-mesh reaches its complete counter clockwise cycle at 7870 time steps. From these results, the characteristics of E_x' and E_y' waveforms in a rotating environment are presented.

Figures 10(a) and 10(b) show the observed waveform for E_x' and H_z' in two different directions which in counter clockwise and clockwise rotation. These numerical results indicate the characteristics of the EM field in both directions. Hence, the analytical results show the capability of this numerical approach in solving moving boundary problems in any environment.
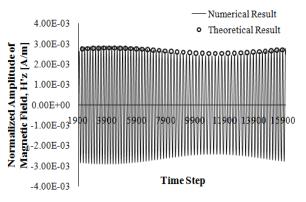

Fig. 8. Comparison of the theoretical and the numerical result for the normalized amplitude of the magnetic field, $H_z' (A/m), v = 2.73 \times 10^7 (ms^{-1})$.

Table 1: The comparison of the normalized amplitude of magnetic field, $H'_z(A/m)$

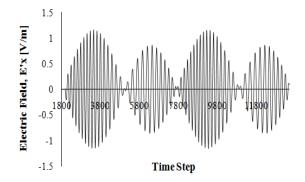|	Rotated towards the incident wave	Rotated away from the incident wave
Numerical (H'_z/H_0)	0.002790	0.002530
Theoretical (H'_z/H_0)	0.002908	0.002434
Absolute Error	0.00012	0.00010

Fig. 9(a). Modulation of the received waveform for electric field, $E'_x(V/m), v = 6.81 \times 10^7 (ms^{-1})$.
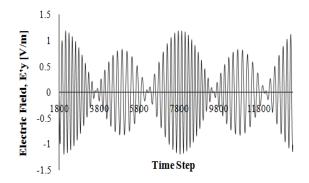

Fig. 9(b). Modulation of the received waveform for electric field, $E'_y(V/m), v = 6.81 \times 10^7 (ms^{-1})$.

V. CONCLUSION

The novel approach based on FDTD method with the overset grid generation method and the Lorentz transformation for the analysis of the EM field in a rotating body is presented. The transition of TE waveforms in amplitude and phase when the rotating observation point strikes the input wave are shown. The characteristic of the EM field in
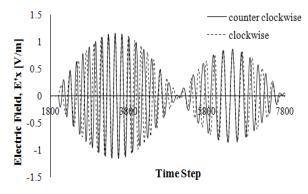

Fig. 10(a). Modulation of electric field, $E'_x(V/m), v = 6.81 \times 10^7 (ms^{-1})$ in counter clockwise and clockwise rotation.
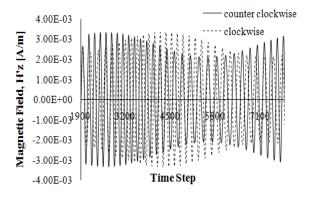

Fig. 10(b). Modulation of magnetic field, $H'_z(A/m), v = 6.81 \times 10^7 (ms^{-1})$ in counter clockwise and clockwise rotation.

counter clockwise and clockwise rotation is analyzed. This approach has shown its advantage over higher velocity cases. The accuracy of this approach has been numerically verified by comparison with the theoretical results. This approach provides a potentially strong numerical support for developing high-frequency devices which comprise a body having a rotational axis.

REFERENCES

[1] G. M. Rebeiz, *RF MEMS Theory, Design and Technology*, John Wiley & Sons Publication, 2003.

[2] V. K. Varadan K. J. Vinoy, and K. A. Jose, *RF MEMS and Their Applications*, John Wiley & Sons Publication, 2003.

[3] A. Freni, C. Mias, and R. L. Ferrari "Finite Element Analysis of Electromagnetic Wave

Scattering by a Cylinder Moving Along its Axis Surrounded by a Longitudinal Corrugated Structure," *IEEE Trans. On Magnetics*, vol. 32, no. 3, pp. 874-877, 1966.

[4] F. Harfoush, A. Taflove, G.A. Kriegsmann "A Numerical Technique for Analyzing Electromagnetic Wave Scattering from Moving Surfaces in One and Two Dimensions," *IEEE Trans. On Antennas and Propagation*, vol. 37, no. 1, pp. 55-63, 1989.

[5] M. J. Inman, A. Z. Elsherbeni, and C. E. Smith, "Finite Difference Time Domain Technique for the Simulation of Moving Objects," *Applied Computational Electromagnetic Society (ACES) Journal,* vol. 20, no. 1 pp. 13-16, 2005.

[6] F. J. Bueche and D. Jerde, *Principles of Physics*, McGraw-Hill Inc, 1994.

[7] G. Desquesnes, M. Terracol, E. Manoha, and P. Sagaut, "On the Use of a High Order Overlapping Grid Method for Coupling in CFD/CAA," *Journal of Computational Physics*, vol. 220, no. 1, pp. 355-382, 2006.

[8] R. Koomullil, G. Cheng, B. Soni, R. Noack, and N. Prewitt, "Moving-Body Simulations Using Overset Framework with Rigid Body Dynamics," *Mathematics and Computers in Simulation*, vol. 78, no. 5-6, pp. 618-626, 2008.

[9] H. Iwamatsu and M. Kuroda, "Over Set Grid Generation Method Coupled with FDTD Method while Considering the Doppler Effect," *IEEJ Trans FM*, vol. 129, no. 10 pp. 699-703, 2009.

[10] L. Rispal and U. Schwalke, "Carbon: The Future of Nanoelectronics," *Proc. of the 2009 International Conference on Signals, Circuits and Systems*, 2009.

[11] P. Russer and N. Fitcher, "Nanoelectronics in Radio-Frequency Technology" *IEEE Microwave Magazine*, vol. 11, no. 3, pp. 119-135, 2010.

[12] J. F. Thompson, B. K. Soni, and Nigel P. Weatherill, *Handbook of Grid Generation*, CRC Press, 1998.

[13] J. V. Bladel, *Relativity and Engineering*, Springer-Verlag, Berlin, 1984.

[14] J. A. Stratton, *Electromagnetic Theory*, The IEEE Press Series on Electromagnetic Wave Theory, Wiley-Interscience, 2007.

[15] A. Taflove and Susan C. Hagness, *Computational Electrodynamics: The Finite-Difference Time-Domain Method 3rd Ed.*, Artech House, Antennas and Propagation Library, 2005.

[16] M. N. Sadiku, *Numerical Techniques in Electromagnetics 2nd Ed.*, CRC Press, 2000.

[17] G. Mur, "Absorbing Boundary Conditions for the Finite-Difference Approximation of the Time-Domain Electromagnetic-Field Equations," *IEEE Transactions on Electromagnetic Compatibility*, vol. EMC-23, no. 4, 1981.

[18] J. V. Bladel, *Electromagnetic Fields(Second Edition)*, The IEEE Press Series on Electromagnetic Wave Theory, Wiley-Interscience, 2007.

[19] S. R. Borkar and R. F. H. Yang "Reflection of Electromagnetic Waves from Oscillating Surfaces," *IEEE Trans. on Antennas and Propagation*, vol. 23, no. 1, pp. 122-127, 1975.

Shafrida Sahrani received her B.E. degree and M.E. degree in Information Networks from Tokyo University of Technology, Tokyo, Japan in 2005 and 2007, respectively. She is currently on study leave from the Universiti Malaysia Sarawak, Malaysia and now working toward Ph.D. degree at Tokyo University of Technology, Tokyo, Japan.

Hiroshi Iwamatsu received the B.E. degree, M.E. degree and D.E. degree in Information Networks from Tokyo University of Technology, Tokyo, Japan, in 2005, 2007, and 2010, respectively. Now, he is a Post-Doctoral researcher at Nihon University, Tokyo, Japan.

Michiko Kuroda Professor Michiko Kuroda received the B. E. degree in Electrical Engineering from Shizuoka University, Shizuoka, Japan and the M. E. and D. E. in Electrical Engineering from Waseda University, Tokyo, Japan. She became an Associate Professor at Tokyo

University of Technology in 1990. Since 1998, she has been a professor at the department of Information Networks. Since 2004, she has been a professor at Scholl of Computer Science. Since 1994, she has been a Correspondent of URSI (International Union of Radio Science) in Japan. Her research interests are electromagnetic theory, and numerical methods including FDTD method and grid generation method. She proposed this novel numerical method for the analysis of the moving boundary problems and its application for the analysis of MEMS devices. Dr. Kuroda is a senior member of the IEEE and a member of ACES, IEICE, and IEEJ.